

Electronic Supplementary Information

Spiroguanidine rhodamines as fluorogenic probes for lysophosphatidic acid

Lei Wang,^a Martha Sibrian-Vazquez,^a Jorge O. Escobedo,^a Jialu Wang,^a
Richard G. Moore^b and Robert M. Strongin^{a,*}

CONTENTS:	Page
Absorbance and fluorescence measurements	S3
Figure S1. Absorption spectra of 5 μM solutions of 1 and 2 .	S3
Figure S2. Excitation and emission spectra of 5 μM solutions of 1 and 2 .	S3
Figure S3. Excitation and emission spectra of 2 and 2 in the presence of LPA 14:0, 16:0, 18:0 and 18:1.	S4
Figure S4. Fluorescence emission intensity of 2 alone and in the presence of LPA 14:0, 16:0, 18:0, 18:1 over time.	S4
Figure S5. Fluorescence emission intensity of 2 and 2 -LPA in CHCl_3 solutions with variable DMSO content.	S5
Table S1. Spectroscopic properties of 1 and 2 in EtOH.	S5
LC-MS/MS LPA analysis	S6
LPA standard solution preparation	S6
Figure S6. Job's plot for the complex formed between 2 and LPA16:0.	S6
Figure S7. Calibration curves of LPA using the LC-ESI/MS/MS method.	S7
Table S2. Statistical values obtained for the individual LPA species in the LC-ESI/MS/MS method.	S7
Figure S8. LC-ESI/MS/MS chromatography of a 10 μM standard mixture of LPA.	S8
Figure S9. Calibration curve derived from a solution of 2 (10 μM) upon titration with LPA. Ex/Em = 550 nm/570 nm; solvent system: CHCl_3 :DMSO 95:5.	S8
Scheme S1. Equilibria between spirocyclic and open forms of spiroguanidine rhodamines 1 and 2 .	S9
Figure S10. Double reciprocal plot of $1/(I-I_0)$ vs. $1/[2]$ to calculate the binding constant K_a of 2 to LPA.	S10
Figure S11. Emission spectra of 10 μM 2 upon titration with LPA.	S10
Synthesis of 1 and 2	S11
Figure S12. ^1H -NMR spectrum of 4 in CDCl_3 .	S15
Figure S13. ^{13}C -NMR spectrum of 4 in CDCl_3 .	S15
Figure S14. ^1H -NMR spectrum of 5 in CDCl_3 .	S16
Figure S15. ^{13}C -NMR spectrum of 5 in CDCl_3 .	S16
Figure S16. ^1H -NMR spectrum of 1 in $\text{DMSO}-d_6$.	S17
Figure S17. ^{13}C -NMR spectrum of 1 in $\text{DMSO}-d_6$.	S17

Figure S18. ^1H -NMR spectrum of 8 in CDCl_3 .	S18
Figure S19. ^{13}C -NMR spectrum of 8 in CDCl_3 .	S18
Figure S20. ^1H -NMR spectrum of 2 in $\text{DMSO}-d_6$.	S19
Figure S21. ^{13}C -NMR spectrum of 2 in $\text{DMSO}-d_6$.	S19
Figure S22. ESI-MS of 4 .	S20
Figure S23. ESI-MS of 5 .	S20
Figure S24. ESI-MS of 1 .	S21
Figure S25. ESI-MS of 8 .	S21
Figure S26. ESI-MS of 2 .	S22
Figure S27. Energy-Minimized structure of 2 in the presence of LPA.	S22
References	S23

Absorbance and fluorescence measurements

UV Absorbance measurements were performed on a Cary Eclipse™ 50 Bio UV-Vis Spectrophotometer. Fluorescence measurements were performed on a Cary Eclipse™ Fluorescence Spectrophotometer (Agilent Technologies). Fluorescence spectra were recorded at an excitation/emission wavelength of 550 nm/570 nm with excitation and emission bandwidths set at 5 nm.

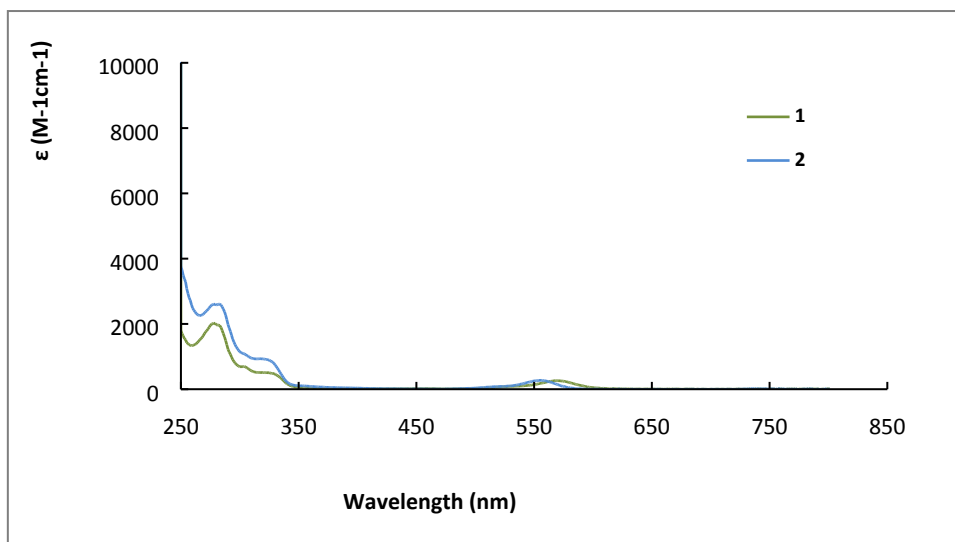


Figure S1. Absorption spectra of 5 μ M solutions of **1** and **2** in CHCl_3 :DMSO 9:1.

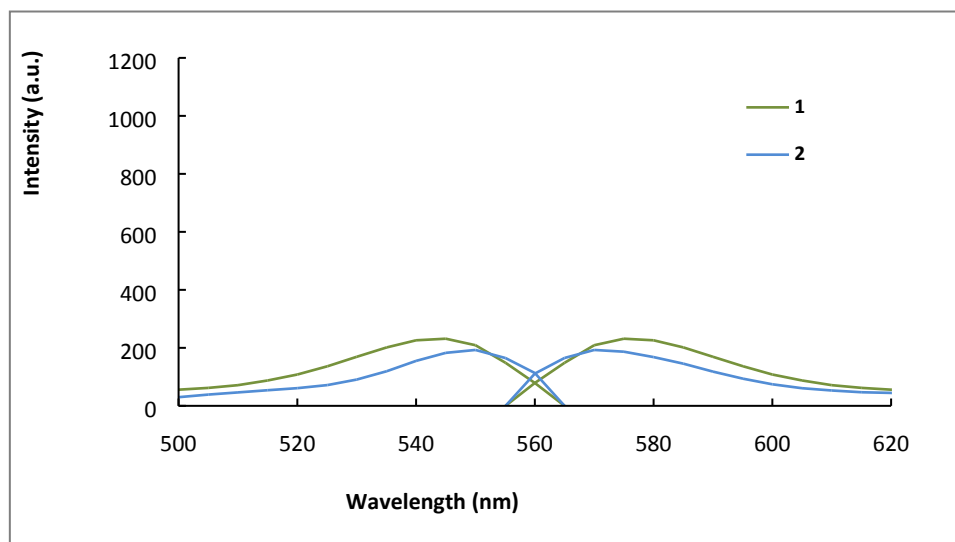


Figure S2. Excitation and emission of 5 μ M solutions of **1** and **2**. Ex/Em = 550 nm/570 nm. solvent system: CHCl_3 : DMSO 9:1.

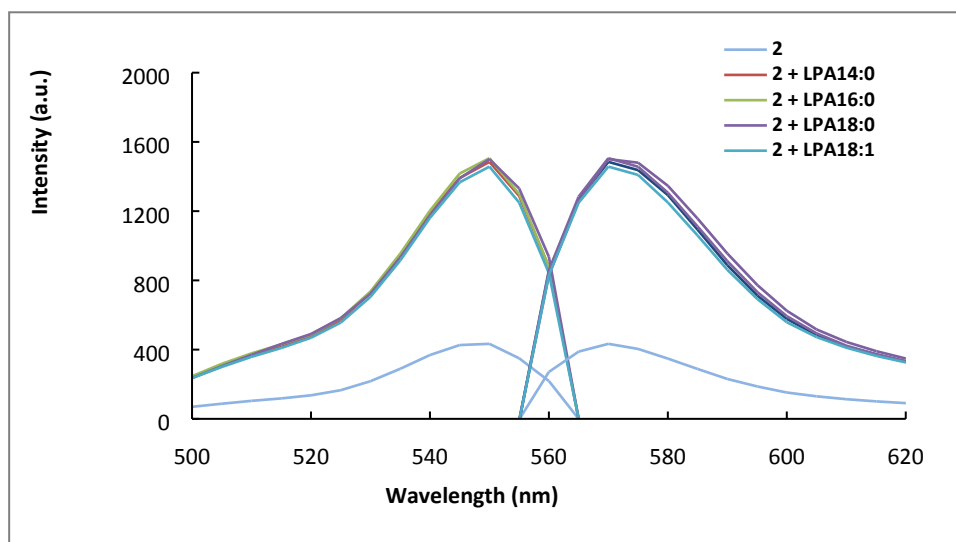


Figure S3. Excitation and emission spectra of **2** and **2** in the presence of LPA 14:0, 16:0, 18:0 and 18:1. Ex/Em = 550 nm/570 nm; final probe concentration: 10 μ M; final LPA concentration: 10 μ M; solvent system: CHCl₃:DMSO 9:1.

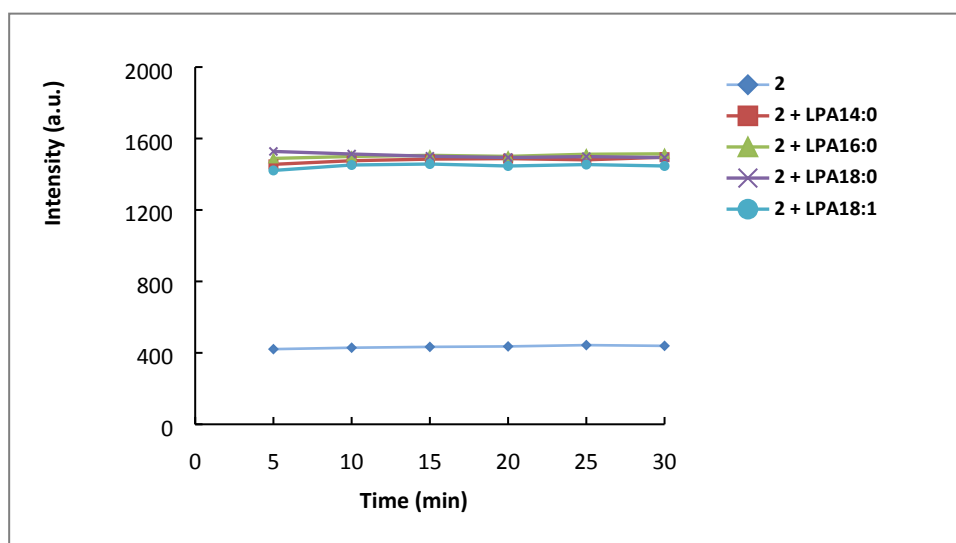


Figure S4. Fluorescence emission intensity of **2** alone and in the presence of LPA 14:0, 16:0, 18:0, 18:1 over time. Ex/Em = 550 nm/570 nm; final probe concentration: 10 μ M; final LPA concentration: 10 μ M; solvent system: CHCl₃:DMSO 9:1.

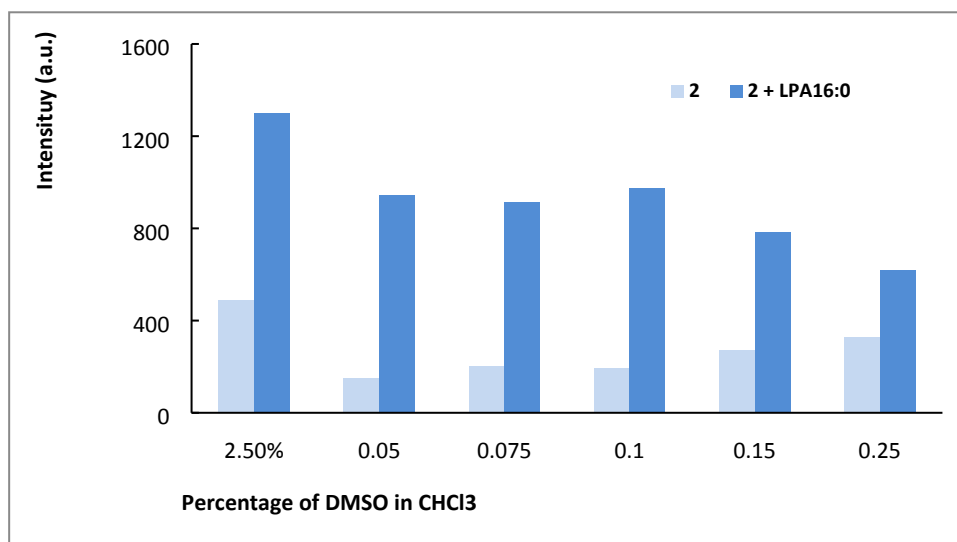


Figure S5. Fluorescence emission intensity of **2** and **2**-LPA in CHCl₃ solutions with variable DMSO content. Ex/Em = 550 nm/570 nm; probe concentration: 5 μ M; LPA16:0 concentration: 10 μ M.

Table S1. Spectroscopic properties of **1** and **2** in EtOH.

	1	2
λ_{max} absorbance (nm)	560	560
λ_{max} emission (nm)	570	570
ϵ (cm ⁻¹ •M ⁻¹)	695	1,026
ϕ	0.31	0.39

LC-MS/MS LPA analysis

LPA separation was carried out on a Luna C8 (50×2 mm, $3 \mu\text{m}$) column at 40°C with an injection volume of $10 \mu\text{L}$. The mobile phase consisting of a mixture of MeOH:formic acid (10 mM , $\text{pH } 2.5$) $9:1$ was delivered at a flow rate of 0.4 mL/min . Ions were created in the negative ion mode setting the sprayer voltage at 3.0 kV and the ion source temperature at 300°C .

LPA standard solution preparation

LPA 14:0, 16:0, 18:0, 18:1 and 20:4 in the acid form were obtained by following the SPE procedure developed by Wang *et al.*¹ as follows: 5 mg of the corresponding LPA (sodium or ammonium) salt is dissolved in 3 mL of HPLC grade water. The solution is acidified by addition of $50 \mu\text{L}$ of $85\% \text{ H}_3\text{PO}_4$. An SPE cartridge (Waters OASISTM HLB 3 cc , 400 mg , $30 \mu\text{m}$) is preconditioned with 6 mL MeOH, followed by 3 mL H_2O . The acidified LPA solution is loaded onto the cartridge and rinsed with 3 mL H_2O followed by 1 mL CHCl_3 . The SPE cartridge is dried by applying a stream of N_2 , and LPA is eluted with 4 mL of MeOH. The solvent is evaporated and the residue reconstituted in 5 mL MeOH.

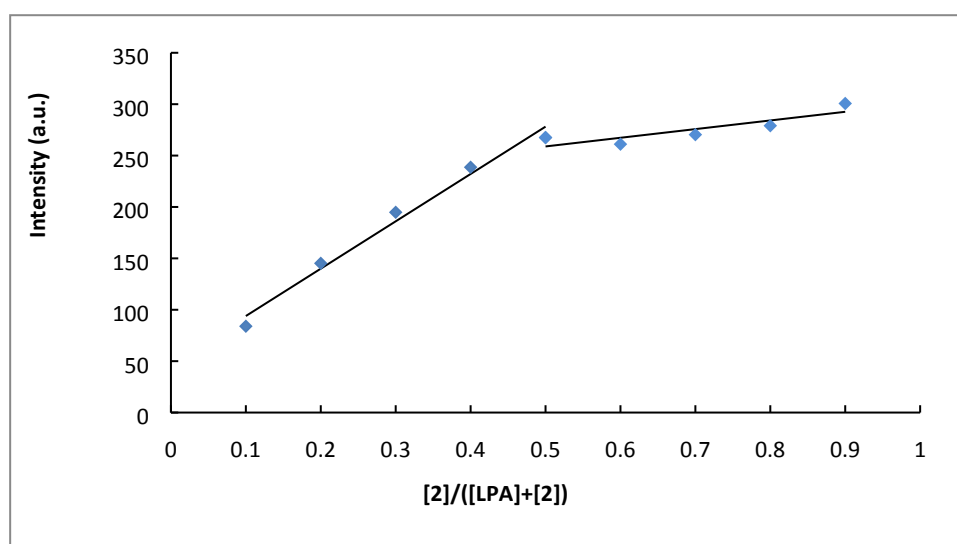


Figure S6. Job's plot for the complex formed between **2** and LPA16:0. $[\mathbf{2}] + [\text{LPA16:0}] = 10 \mu\text{M}$. Ex/Em = $550 \text{ nm}/570 \text{ nm}$; solvent system: $\text{CHCl}_3:\text{DMSO } 95:5$.

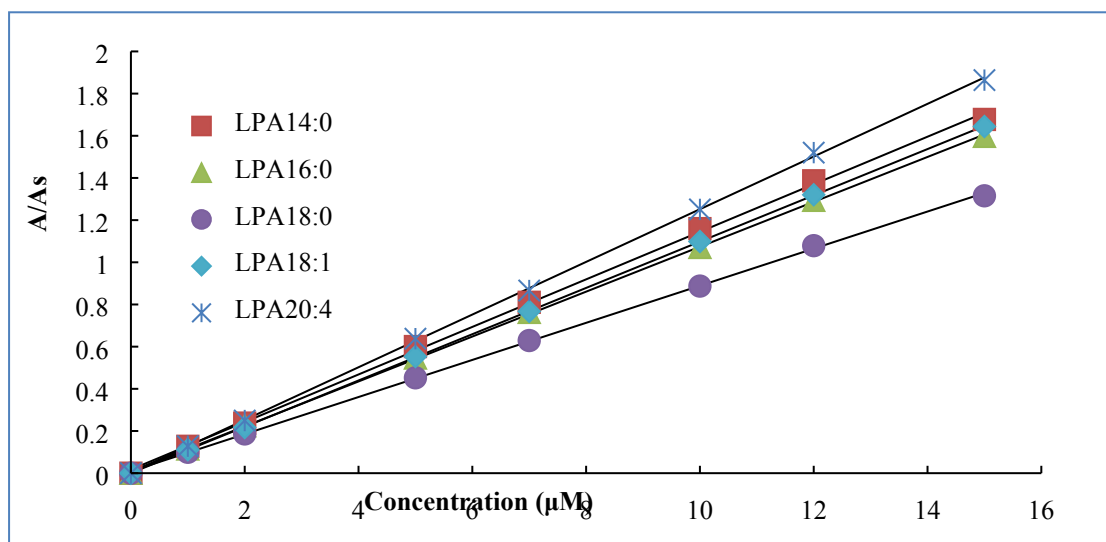


Figure S7. Calibration curves of LPA using the LC-ESI/MS/MS method. The area ratio (A/As) is the peak area of individual LPA divided by the peak area of the internal standard (LPA 17:0). Data points represent the average of 3 runs.

Table S2. Statistical values obtained for the individual LPA species in the LC-ESI/MS/MS method ($n=3$)

LPA species	Retention time (min)	Linear range (μM)	R^2	LOD (μM)
14:0	3.21	0-15	0.99918	0.02499
16:0	4.09	0-15	0.99987	0.01594
18:0	5.51	0-15	0.99970	0.03968
18:1	4.48	0-15	0.99998	0.01966
20:4	3.71	0-15	0.99977	0.00840

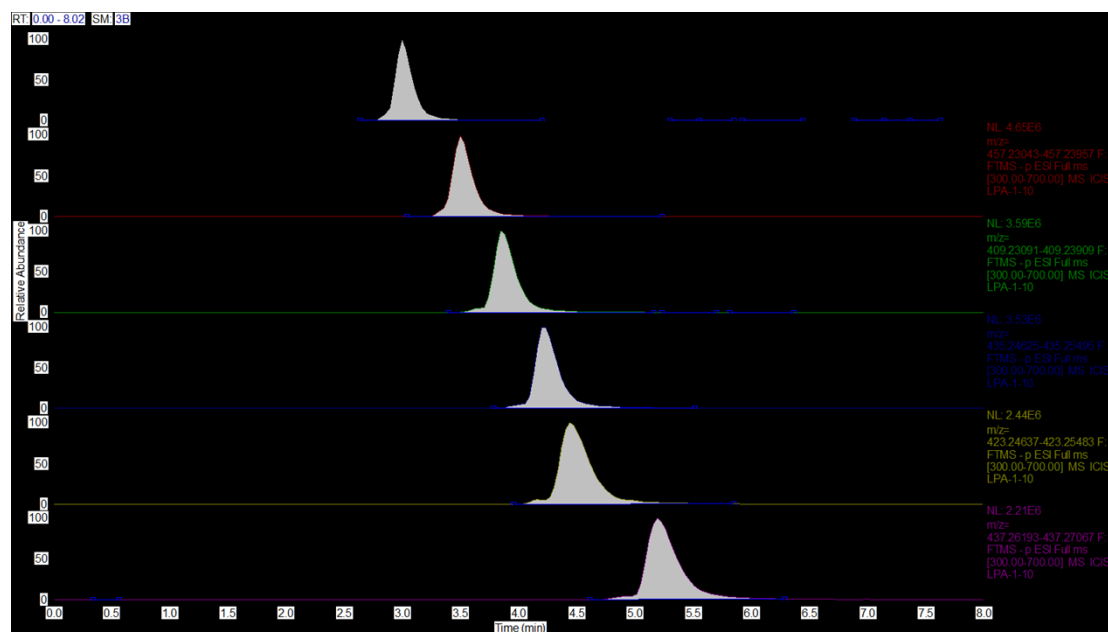


Figure S8. LC-ESI/MS/MS chromatography of a 10 μ M standard mixture of LPAs. Column: LunaTM C-8 (50 \times 2 mm, 3 μ m) at 40 $^{\circ}$ C. Injection volume: 10 μ L. Mobile phase: MeOH:aqueous formic acid (pH 2.5) 9:1 at a flow rate of 0.4 mL/min. Sprayer voltage; 3.0 kV, capillary temperature at 300 $^{\circ}$ C. Parent and daughter ions were detected in the negative ion mode.

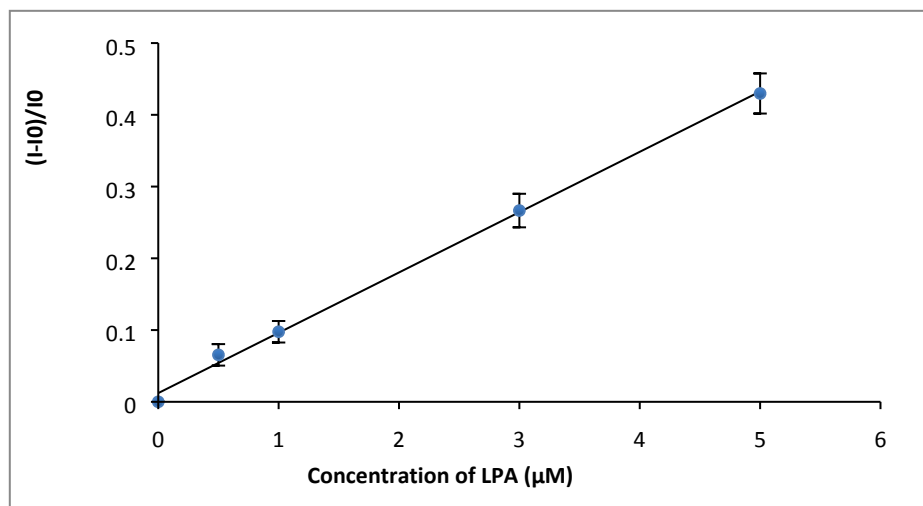
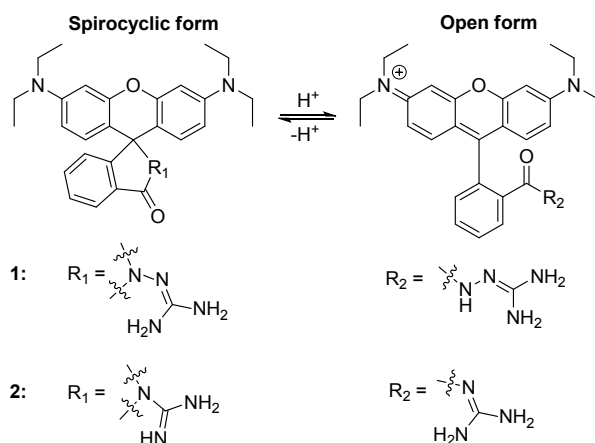


Figure S9. Calibration curve derived from a solution of **2** (10 μ M) upon titration with LPA. Ex/Em = 550 nm/570 nm; solvent system: CHCl₃:DMSO 95:5.



Scheme S1. Equilibria between spirocyclic and open forms of spiroguanidine rhodamines **1** and **2**.

For a binding ratio of 1:1, equations (1) and (2) were used. A double reciprocal curve was plotted (**Figure S10**), and from the regression equation, $K_a = 4.622 \times 10^5 \text{ M}^{-1}$ ($R^2 = 0.9910$).

$$\frac{1}{I - I_0} = \frac{1}{I_\infty - I_0} + \frac{1}{I_\infty - I_0} \times \frac{1}{K_a} \times \frac{1}{[Probe\ 2]} \quad (1)$$

$$K_a = \frac{\text{Intercept}}{\text{Slope}} \quad (2)$$

I_0 , I , I_∞ are the fluorescence intensities of **2** in absence of, in the presence of, and at a concentration corresponding to saturation, respectively, of LPA. K_a is the binding constant.

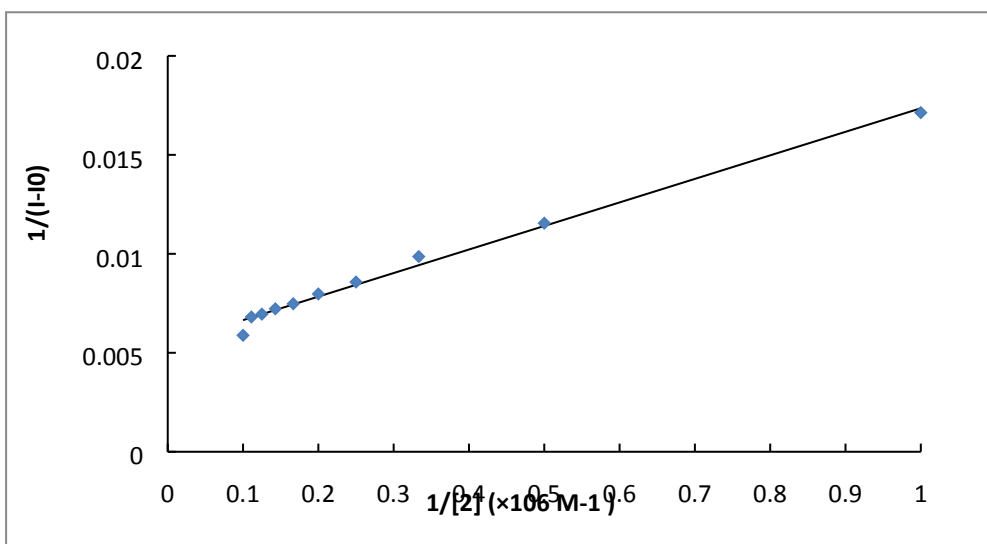


Figure S10. Double reciprocal plot of $1/(I-I_0)$ vs. $1/[2]$ to calculate the binding constant K_a of **2** to LPA; LPA16:0 concentration: 5 μM .

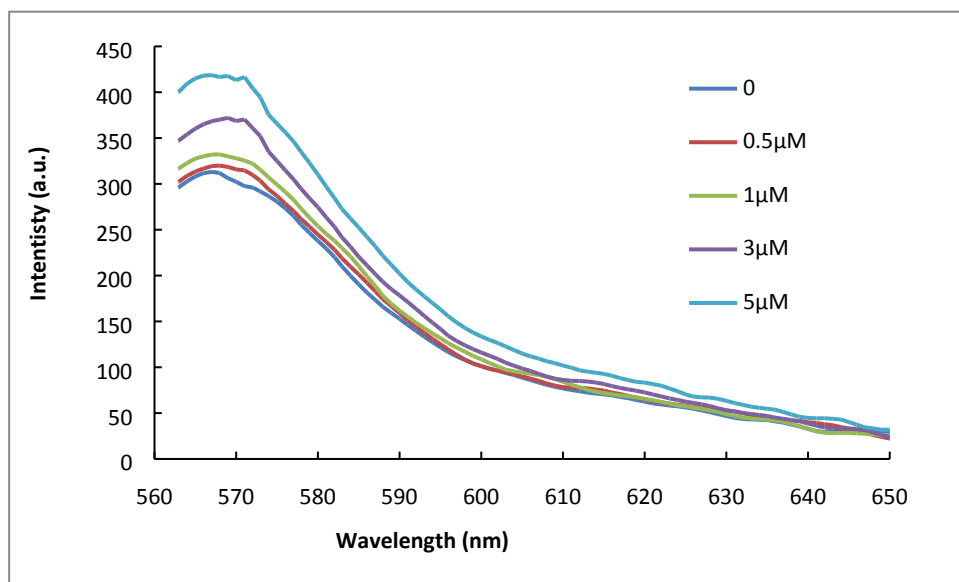


Figure S11. Emission spectra of 10 μM **2** upon titration with LPA. Ex/Em = 550 nm/570 nm; solvent system: CHCl_3 :DMSO 95:5.

Synthesis of 1 and 2.

Rhodamine B, rhodamine B base, 1,3-*bis*-*boc*-2-methyl-2-thiopseudourea, sodium methoxide solution (0.5 M in MeOH), and 1,3-*bis*-(*tert*-butoxycarbonyl)guanidine were purchased from Sigma-Aldrich. Anhydrous K₂CO₃ and trifluoroacetic acid were purchased from Fisher Scientific. Mercury(II) chloride was purchased from Acros Organics. Lysophosphatidic acids salts were purchased from Avanti Polar Lipids. Silica gel with a pore diameter of 60Å and particle size of 40-63 µm (230 × 400 mesh) was purchased from Sorbent Technologies. All chemicals were used as received without further purification. NMR spectra were recorded on either a ARX-400 or ARX-600 Advance Bruker spectrometer. MS (HRMS, ESI) spectra were obtained at the PSU Bioanalytical Mass Spectrometry Facility on a Thermo Electron LTQ-Orbitrap Discovery high resolution mass spectrometer.

2-amino-3',6'-bis(diethylamino)spiro[isoindoline-1,9'-xanthen]-3-one (4).² To a stirred solution of **3** (Scheme 2, 1 g, 2.1 mmol) in EtOH (60 mL) at rt is added hydrazine monohydrate (98%, 0.6 mL, 12 mmol). The mixture heated at reflux for 12 h. After cooling to rt, the solvent is evaporated under reduced pressure. The solid is dissolved in CHCl₃ (50 mL) and the organic phase is washed with H₂O (3 × 50 mL), followed by drying over anhydrous Na₂SO₄. After filtration and removal of the solvent, the crude product is purified by flash chromatography (CH₂Cl₂:MeOH 97.5:2.5) to afford a yellow oil. Yield: 950 mg (95%). The characterization data is consistent with the literature.²

(E)-tert-butyl(3',6'-bis(diethylamino)-3-oxospiro[isoindoline-1,9'-xanthene]-2-ylamino)(tert-butoxy-carbonylamino) methylenecarbamate (5). To a stirred solution of **4** (290 mg, 0.64 mmol), HgCl₂ (190 mg, 0.70 mmol) and 1,3-*bis*-*boc*-2-methyl-2-thiopseudourea (188 mg, 0.70 mmol) in anhydrous DMF (10 mL) under Ar is added Et₃N (0.45 mL, 3.18 mmol). The suspension is stirred over an ice bath for 2 h, and then at rt for 12h. The mixture is diluted with CHCl₃ and filtered through celite. The filtrate is washed with saturated aqueous NaHCO₃ (25 mL) and H₂O (3 × 25 mL). The organic phase is dried over anhydrous Na₂SO₄. After filtration and removal of solvent, the crude product is purified by flash chromatography (EtOAc:hexane 1:2) to

afford a purple solid with a yield of 410 mg (90%). ¹H-NMR (600 MHz, CDCl₃) δ 1.16 (t, *J* = 6.9 Hz, 12H), 1.37 (s, 9H), 1.38 (s, 9H), 3.33 (m, *J* = 6.8 Hz, 8H), 6.27 (dd, *J* = 32.5, 8.2 Hz, 2H), 6.36 (d, *J* = 14.9 Hz, 2H), 6.77 (s, 1H), 7.10 (t, *J* = 7.3 Hz, 1H), 7.46 (m, 2H), 7.94 (t, *J* = 10.8 Hz, 1H), 9.33 (s, 1H), 11.16 (s, 1H). ¹³C NMR (151 MHz, CDCl₃) δ 12.78, 28.07, 28.35, 44.47, 66.68, 78.80, 83.25, 97.81, 104.55, 108.02, 123.60, 124.19, 128.02, 128.23, 129.03, 133.21, 149.03, 152.35, 153.75, 156.39, 163.56. ESI-MS (*m/z*) for C₃₉H₅₀N₆O₆ [M+H]⁺: calculated 699.3864, observed 699.3932.

1-(3',6'-bis(diethylamino)-3-oxospiro[isoindoline-1,9'-xanthene]-2-yl)guanidine

(1). To a stirred solution of **5** (380 mg, 0.55 mmol) in CH₂Cl₂ (2 mL) is slowly added 4 mL of a TFA:CH₂Cl₂ 1:1 solution. Stirring at rt is continued until the reaction is complete according to TLC analysis. Solvent and excess TFA are evaporated under reduced pressure to afford the trifluoroacetate salt as a dark purple solid. The solid is dissolved in anhydrous MeOH (3 mL). A 0.5 M NaOMe solution (3 mL) is added and the mixture stirred at rt for 1 h. The solvent is evaporated under reduced pressure. The resulting solid is dissolved in CHCl₃ (50 mL) and washed with aqueous saturated NaHCO₃ (25 mL) and H₂O (3 × 25 mL). The organic phase is dried over anhydrous Na₂SO₄. After filtration and removal of the solvent, the crude product is purified by flash chromatography (CH₂Cl₂:MeOH 9:1) to afford a purple solid with a yield of 160 mg (60%). ¹H-NMR (600 MHz, DMSO-*d*₆) δ 1.08 (t, *J* = 7.0 Hz, 3H), 3.30 (q, *J* = 7.1 Hz, 8H), 5.51 (d, *J* = 293.9 Hz, 4H), 6.27 (dd, *J* = 8.9, 2.5 Hz, 2H), 6.30 (d, *J* = 2.5 Hz, 2H), 6.56 (d, *J* = 7.3 Hz, 2H), 6.88 (d, *J* = 6.9 Hz, 1H), 7.42 (m, 2H), 7.71 (d, *J* = 6.5 Hz, 1H). ¹³C-NMR (151 MHz, DMSO-*d*₆) δ 12.49, 43.63, 65.29, 97.15, 105.99, 107.39, 121.78, 123.17, 127.77, 128.72, 130.55, 131.59, 147.93, 152.34, 152.78, 158.53. ESI-MS (*m/z*) for C₂₉H₃₄N₆O₂ [M+H]⁺: calculated 499.2860, observed 499.2846.

***N*-(9-(2-(chlorocarbonyl)phenyl)-6-(diethylamino)-3*H*-xanthen-3-ylidene)-*N*-**

ethylethanaminium (7).³ To a solution of **6** (500 mg, 1.13 mmol) in anhydrous 1,2-dichloroethane (5 mL), is added a solution of POCl₃ (0.26 mL, 2.8 mmol) in 1,2-dichloroethane (5 mL) dropwise over 5 min. The mixture is heated at reflux for 4 h.

After the mixture is cooled to rt, the solvent is evaporated under reduced pressure to yield rhodamine B acyl chloride which is used as is in the next reaction.

(E)-tert-butyl-(3',6'-bis(diethylamino)-3-oxospiro[isoindoline-1,9'-xanthene]-2-yl)methanediylidene-dicarbamate (8). 1,3-bis(tert-butoxycarbonyl)guanidine (290 mg, 1.13 mmol) and K₂CO₃ (0.62 g, 4.5 mmol) are dissolved in anhydrous MeCN (5 mL) under Ar. The crude rhodamine B acyl chloride is dissolved in anhydrous MeCN (5 mL) and added dropwise to the solution over 3 h. After 12 h, the solvent is evaporated under reduced pressure and the residue washed with aqueous saturated NaHCO₃ (25 mL) and H₂O (3 × 25 mL). The combined organic phase is dried over anhydrous Na₂SO₄. After filtration and removal of solvent, the crude product is purified by flash chromatography (EtOAc:hexane 1:2) to afford a yellow solid with a yield of 476 mg (62%). ¹H-NMR (600 MHz, CDCl₃) δ 1.13 (t, *J* = 7.1 Hz, 12H), 1.35 (s, 9H), 1.41 (s, 9H), 3.30 (m, 8H), 6.18 (dd, *J* = 8.8, 2.6 Hz, 2H), 6.30 (d, *J* = 8.8 Hz, 2H), 6.35 (d, *J* = 2.6 Hz, 2H), 7.16 (d, *J* = 7.7 Hz, 1H), 7.51 (m, 1H), 7.58 (td, *J* = 7.5, 1.1 Hz, 1H), 7.94 (d, *J* = 7.6 Hz, 1H), 10.75 (s, 1H). ¹³C-NMR (151 MHz, CDCl₃) δ 12.78, 28.15, 28.18, 44.40, 68.30, 78.74, 81.78, 97.72, 106.68, 107.23, 123.59, 125.09, 127.65, 128.75, 129.20, 135.16, 139.08, 148.97, 150.16, 153.42, 154.20, 156.14, 171.05. ESI-MS (*m/z*) for C₃₉H₄₉N₅O₆ [M+H]⁺: calculated 684.3756, observed 684.3794.

3',6'-bis(diethylamino)-3-oxospiro[isoindoline-1,9'-xanthene]-2-carboximidamide (2). To a stirred solution of **8** (300 mg, 0.44 mmol) in CH₂Cl₂ (2 mL) is added slowly 4 mL of a TFA:CH₂Cl₂ 1:1 solution. Stirring at rt is continued until the reaction is complete based on TLC analysis. Solvent and excess TFA are evaporated under reduced pressure to afford the trifluoroacetate salt as a dark purple solid, which is dissolved in anhydrous MeOH (3 mL). A 0.5 M NaOMe solution (3 mL) is added, and the mixture stirred at rt for 1h. The solvent is evaporated under reduced pressure and the resulting solid is dissolved in CHCl₃ (50 mL), washed with aqueous saturated NaHCO₃ (25 mL) and H₂O (3 × 25mL). The combined organic phases are dried over anhydrous Na₂SO₄. After filtration and removal of solvent, the crude product is purified by flash chromatography (CH₂Cl₂:MeOH 9:1) to afford a light purple solid

with a yield of 110 mg (52%). ^1H -NMR (600 MHz, $\text{DMSO-}d_6$) δ 1.09 (t, $J = 7.0$ Hz, 12H), 3.34 (q, $J = 7.1$ Hz, 8H), 6.42 (dd, $J = 9.0, 2.6$ Hz, 2H), 6.45 (d, $J = 2.5$ Hz, 2H), 6.72 (d, $J = 8.9$ Hz, 2H), 7.01 (d, $J = 7.8$ Hz, 1H), 7.58 (m, 1H), 7.68(m, $J = 1.1$ Hz, 1H), 7.69 (bs, 3H), 7.99 (d, $J = 7.7$ Hz, 1H). ^{13}C -NMR (151 MHz, $\text{DMSO-}d_6$) δ 12.38, 43.69, 79.18, 97.67, 103.08, 108.69, 123.65, 124.39, 124.53, 127.22, 129.43, 136.51, 149.17, 151.72, 153.52, 153.64, 169.01. ESI-MS (m/z) for $\text{C}_{29}\text{H}_{33}\text{N}_5\text{O}_2$ $[\text{M}+\text{H}]^+$: calculated 484.2707, observed 484.2751.

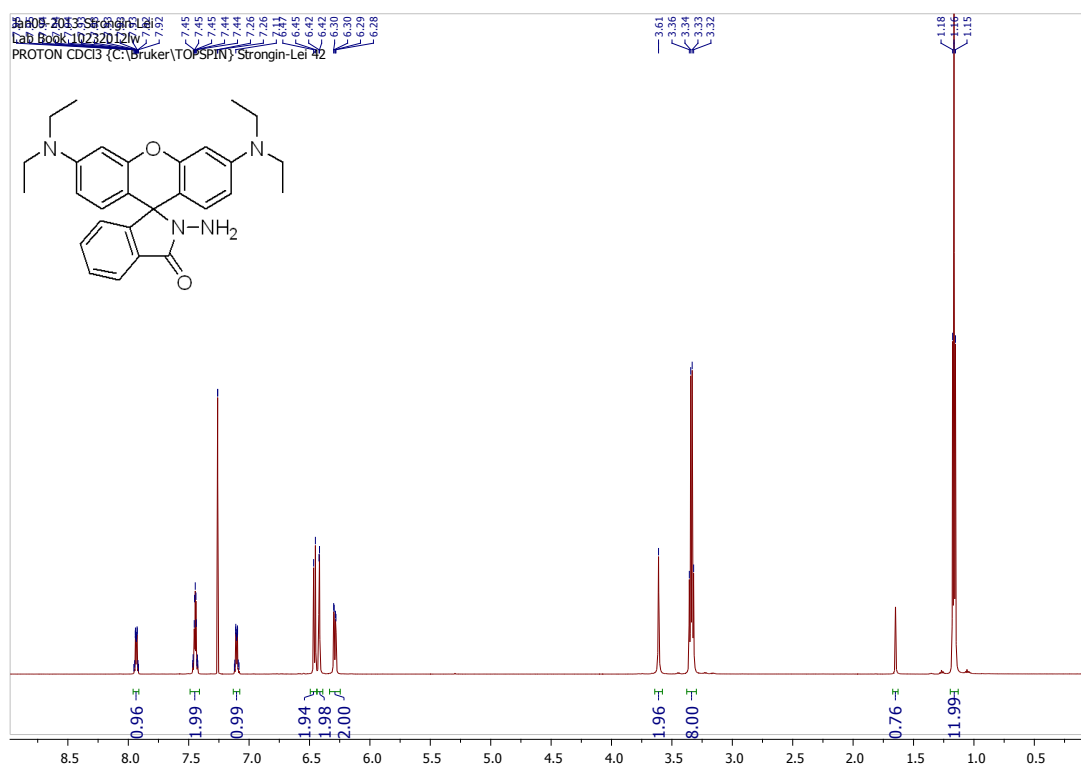


Figure S12. ^1H -NMR spectrum of **4** in CDCl_3 .

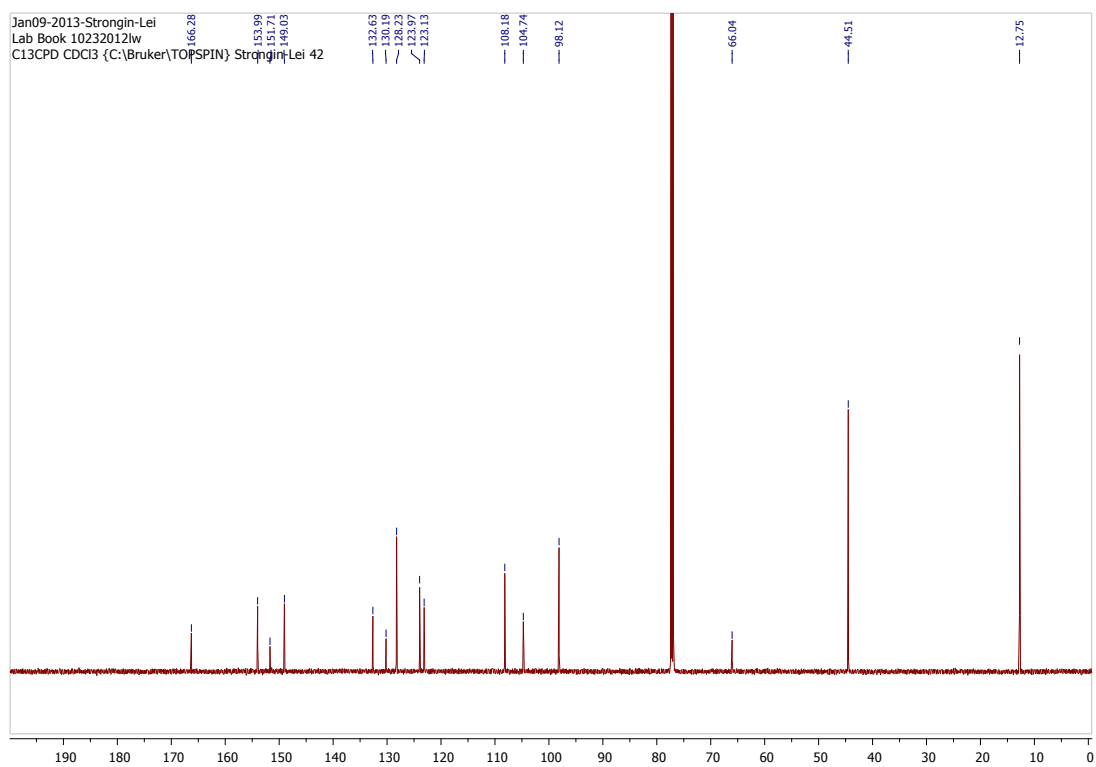


Figure S13. ^{13}C -NMR spectrum of **4** in CDCl_3 .

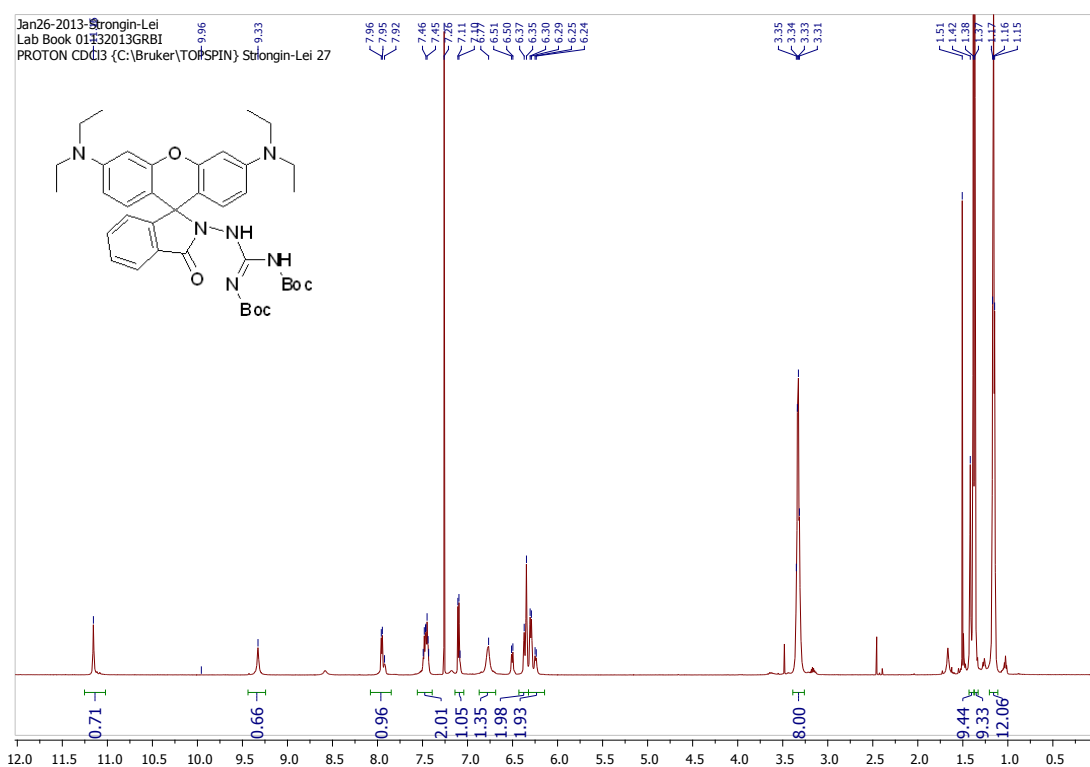


Figure S14. ¹H-NMR spectrum of **5** in CDCl₃.

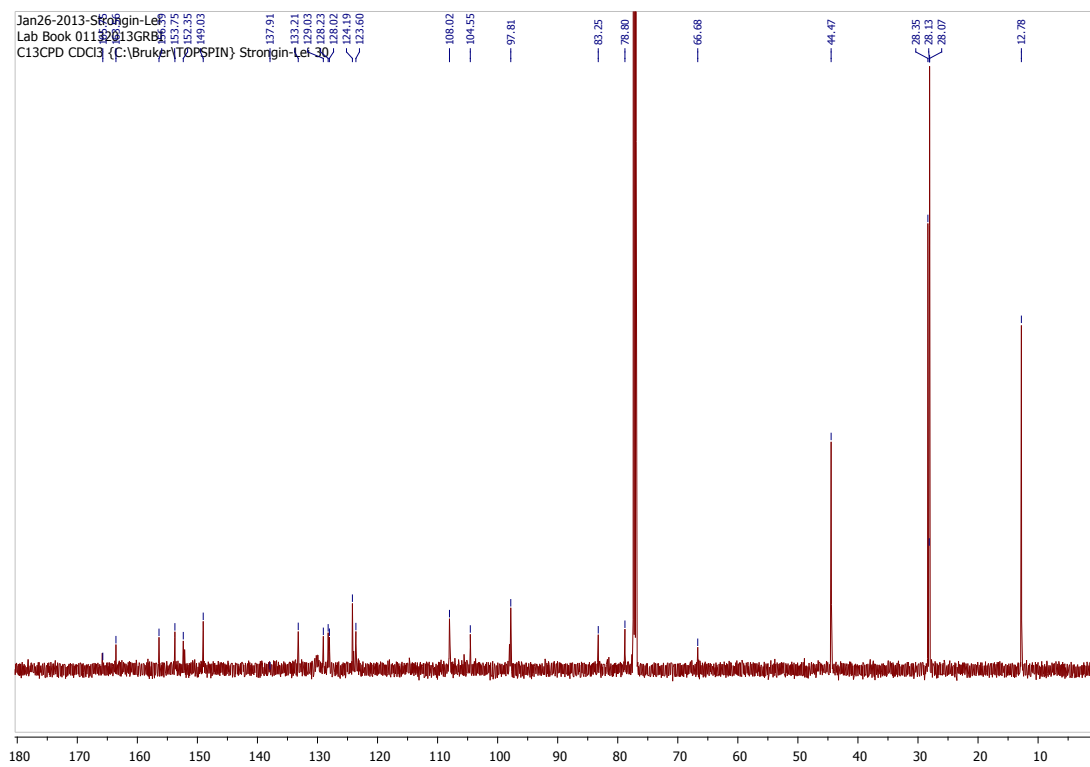


Figure S15. ¹³C-NMR spectrum of **5** in CDCl₃.

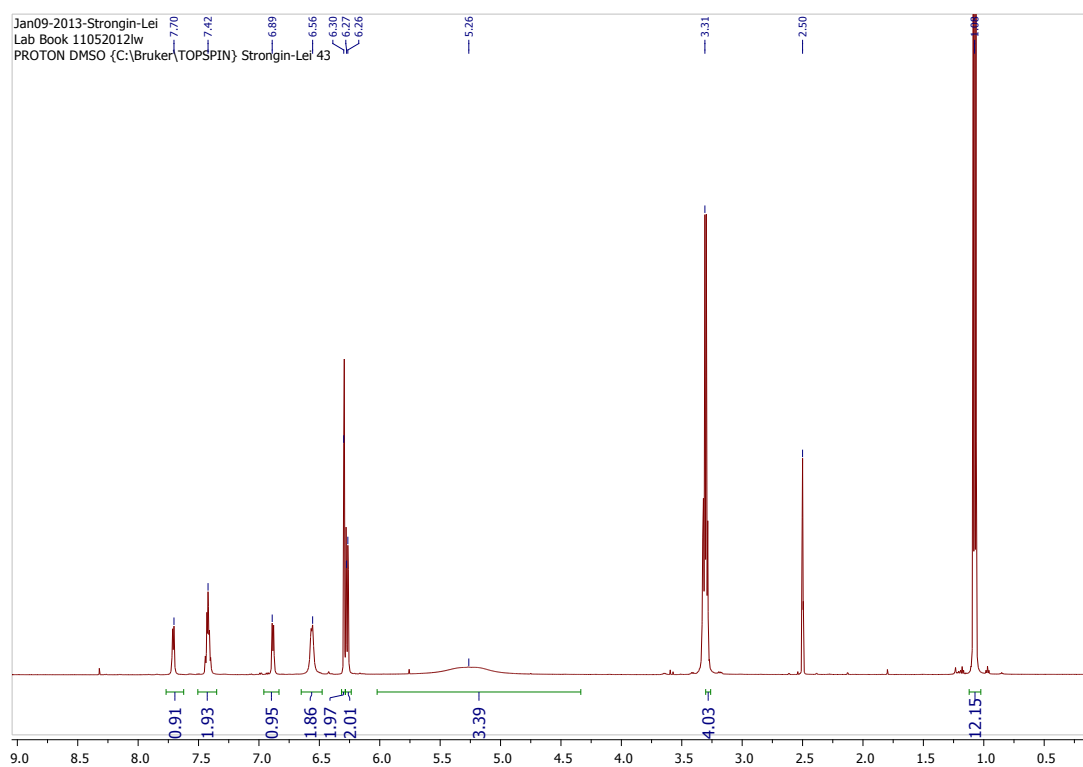


Figure S16. ^1H -NMR spectrum of **1** in $\text{DMSO}-d_6$.

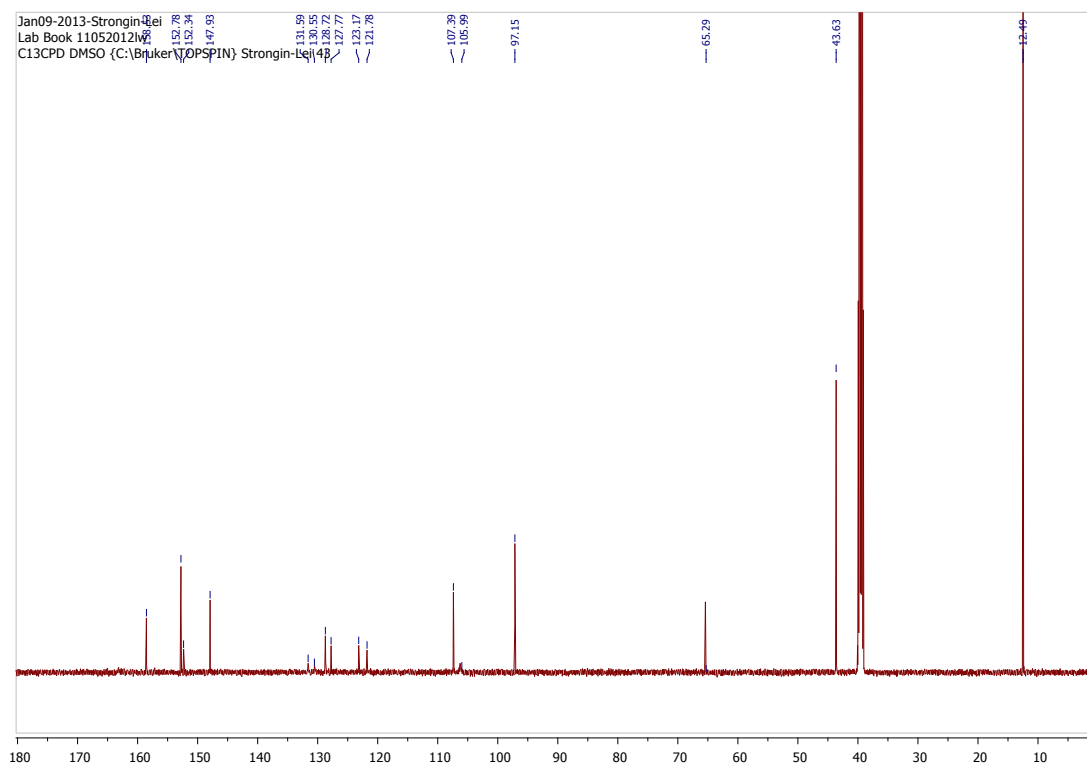


Figure S17. ^{13}C -NMR spectrum of **1** in $\text{DMSO}-d_6$.

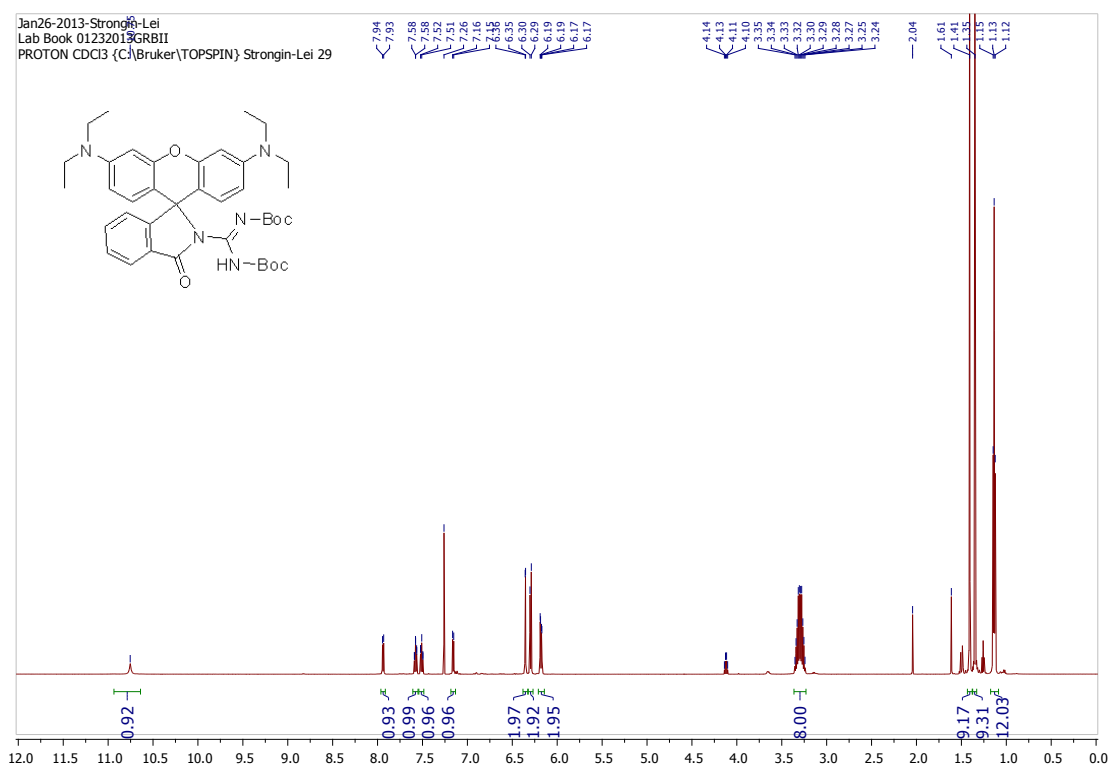


Figure S18. ¹H-NMR spectrum of **8** in CDCl₃.

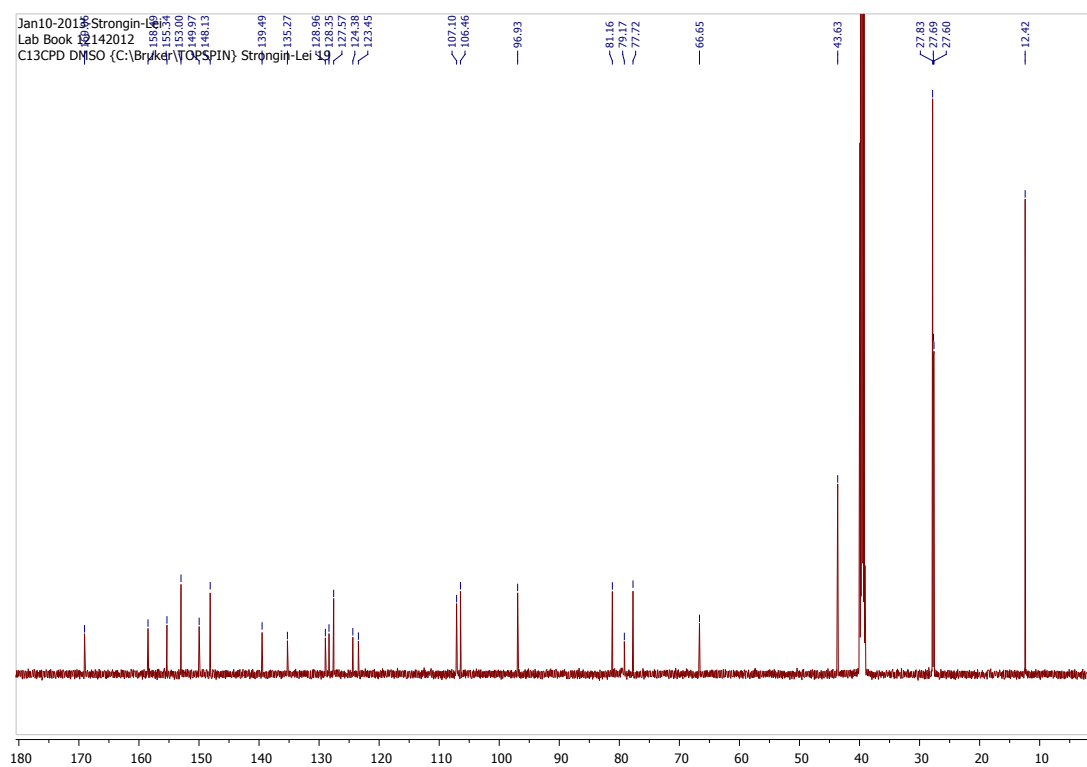
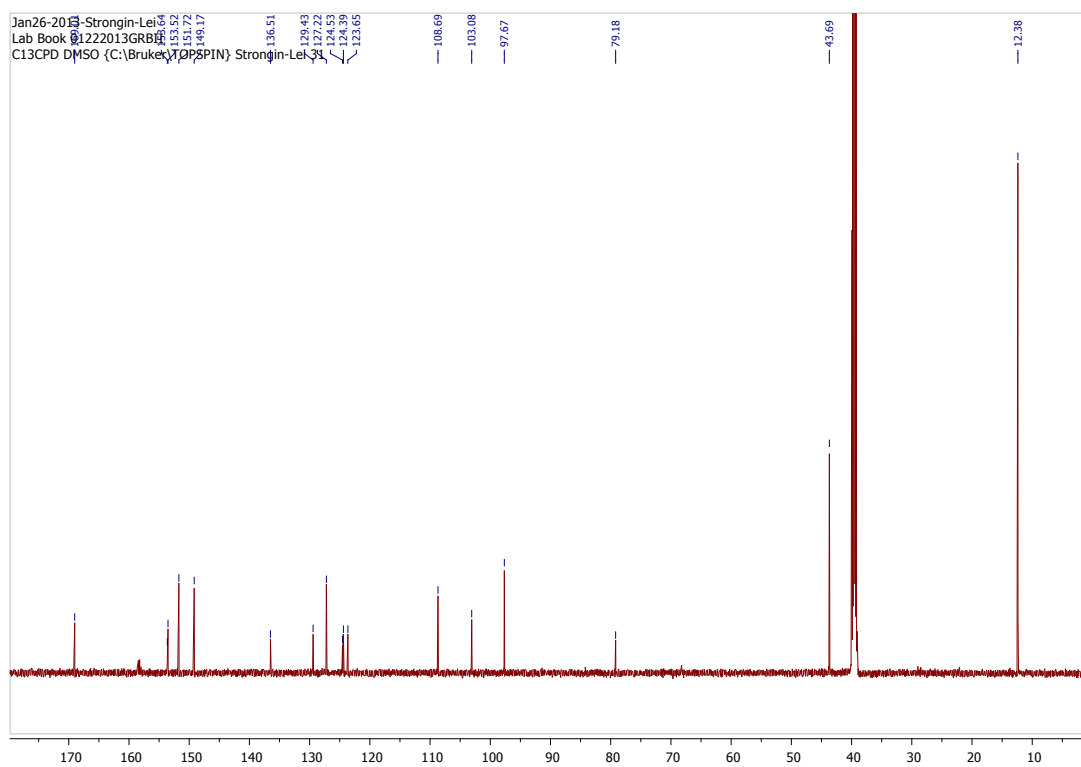
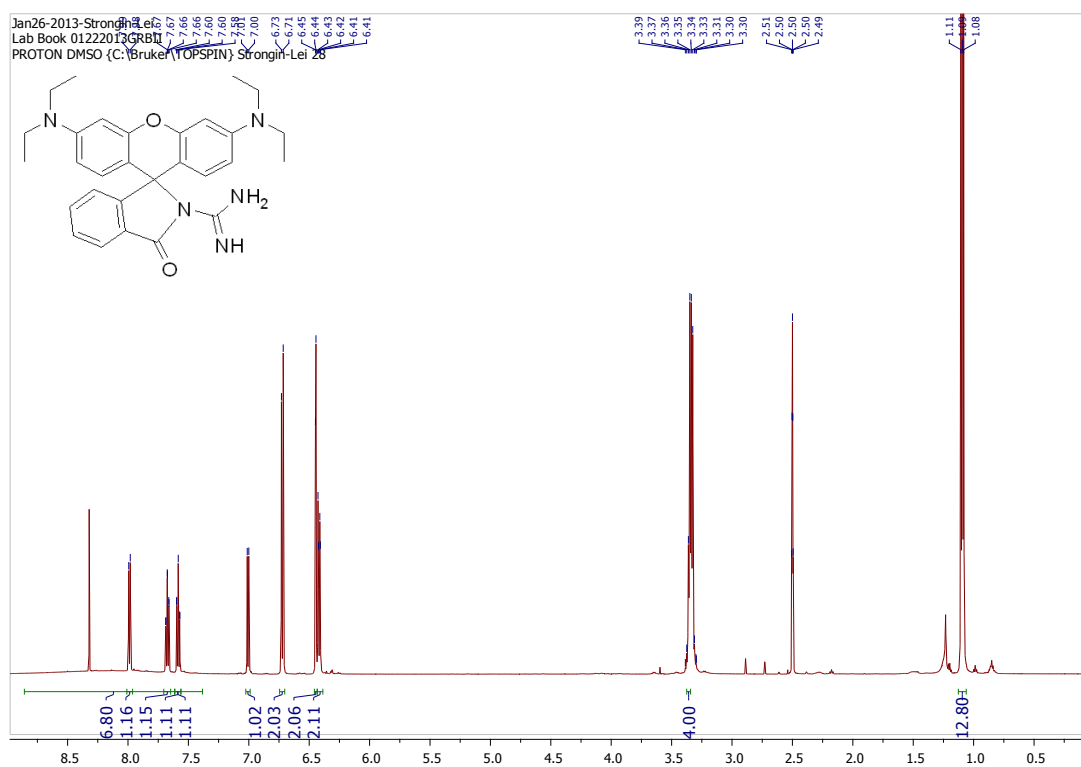


Figure S19. ¹³C-NMR spectrum of **8** in CDCl₃.



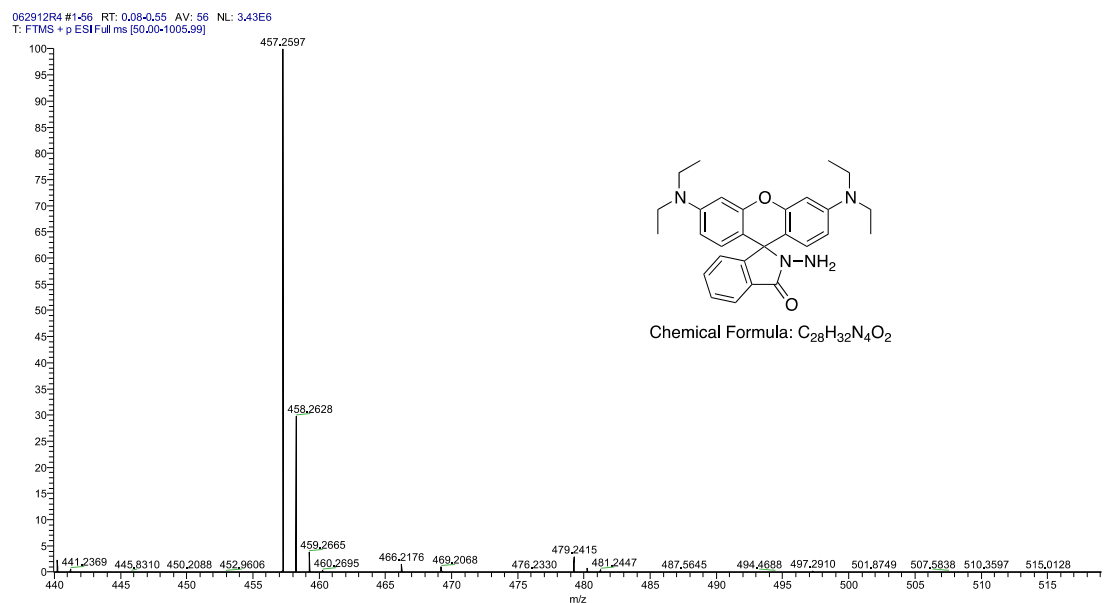


Figure S22. ESI-MS of 4.

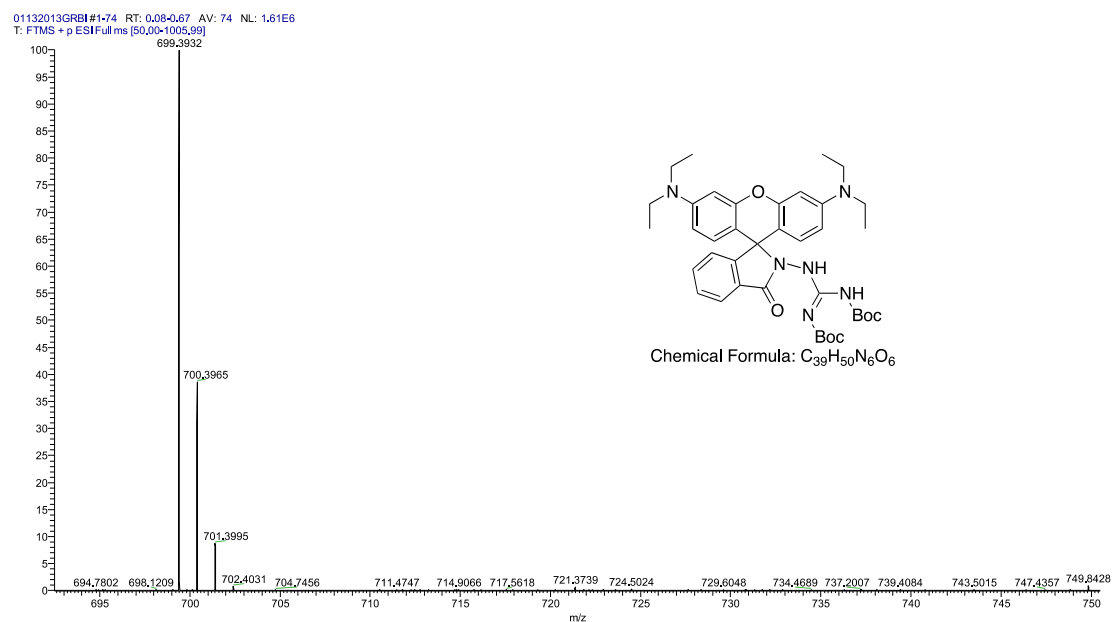


Figure S23. ESI-MS of 5.

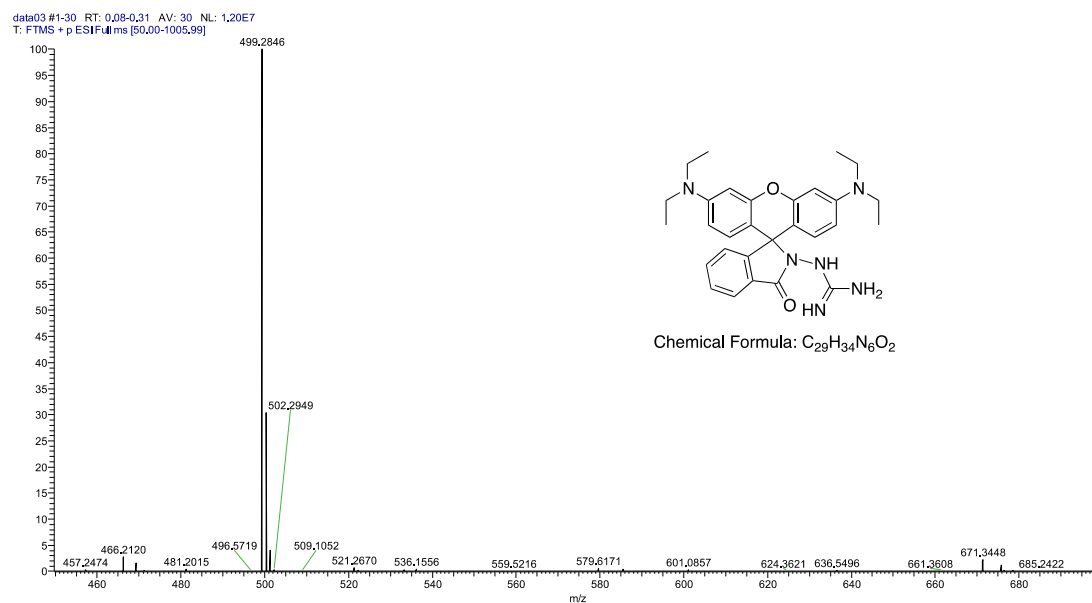


Figure S24. ESI-MS of **1**.

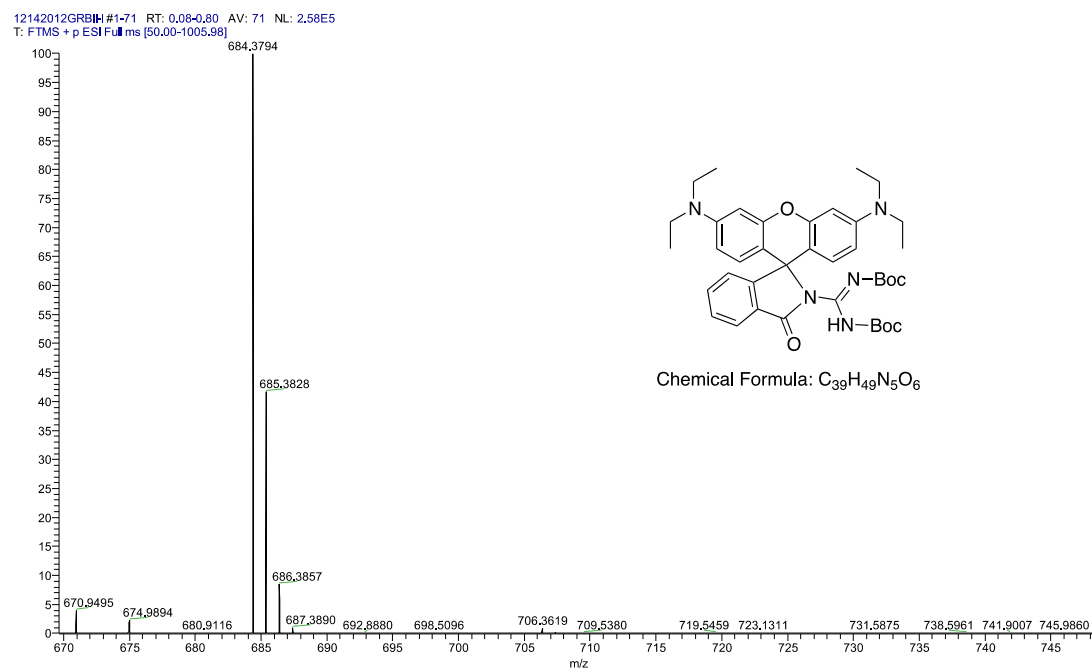


Figure S25. ESI-MS of **8**.

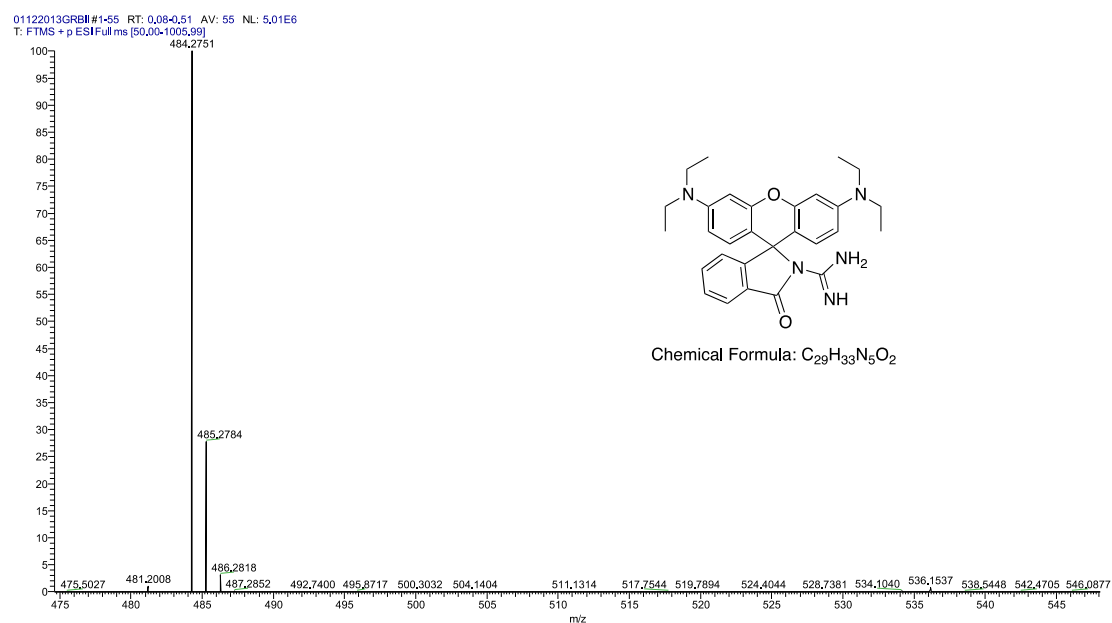


Figure S26. ESI-MS of **2**.

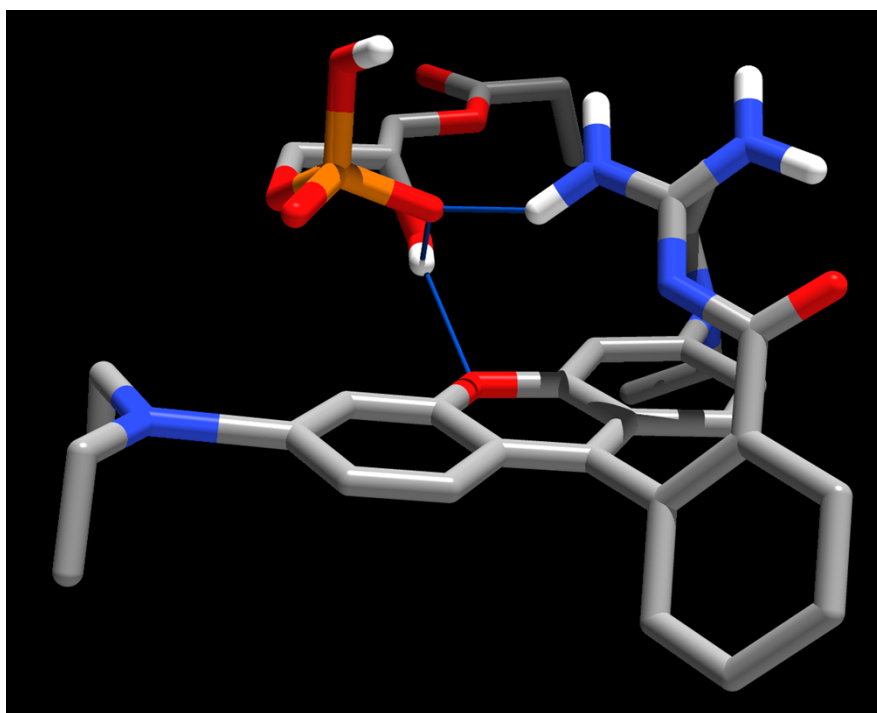


Figure S27. Energy-Minimized structure of **2** in the presence of LPA.

References

1. J. Wang, M. Sibrian-Vazquez, J. O. Escobedo, M. Lowry, L. Wang, Y. H. Chu, R. G. Moore and R. M. Strongin, *Analyst*, 2013, **138**, 6852-6859.
2. X.-F. Yang, X.-Q. Guo and Y.-B. Zhao, *Talanta*, 2002, **57**, 883-890.
3. W. Liu, L. Xu, H. Zhang, J. You, X. Zhang, R. Sheng, H. Li, S. Wu and P. Wang, *Org. Biomol. Chem.*, 2009, **7**, 660-664.

^aDepartment of Chemistry, Portland State University, Portland, OR 97201, USA.

E-

mail: strongin@pdx.edu; Tel: +1-503-725-9724.

^bWomen and Infants Hospital, Brown University, 101 Dudley Street, Providence, RI 02905, USA.

E-

mail: RMoore@wihri.org; Tel: +1-401-453-7520.